www.czasopisma.pan.pl PAN POLSKA AKADEMIA NAUK www.journals.pan.pl

Metrol. Meas. Syst., Vol. XVIII (2011), No. 1, pp. 129-136

PAN POLSKA AKADEMIA NAUK

METROLOGY AND MEASUREMENT SYSTEMS

Index 330930, ISSN 0860-8229

www.metrology.pg.gda.pl

M&MS

DESIGN AND PERFORMANCE OF THE CONVERGING-DIVERGING VORTEX FLOWMETER

Zhiqiang Sun

School of Energy Science and Engineering, Central South University, Changsha 410083, China (zqsun@mail.csu.edu.cn)

Abstract

The converging-diverging structure is introduced to extend the lower limit of measurement of vortex flowmeters. As a compact device, the converging-diverging vortex flowmeter is proposed and designed, and its performance is studied experimentally. It is found that, first of all, an up to 51% extension of the lower measurement limit can be realized through the converging-diverging structure, compared with conventional vortex flowmeters; second, the converging-diverging vortex flowmeter with a trapezoidal bluff body has a larger Strouhal number and smaller pressure loss. The results suggest that the converging-diverging vortex flowmeter provides an alternative device especially suitable for the measurement of low-velocity fluids.

Keywords: vortex flowmeter, converging-diverging structure, lower limit of measurement, Strouhal number, drag coefficient.

1. Introduction

As one of the most promising flow measurement devices, the vortex flowmeter is adopted in many industrial fields and is regarded as an ideal substitute for orifices. Vortex flowmeters are suitable for the measurement of gases, liquids, and even some gas-liquid two-phase flows [1,2]. Performances of vortex flowmeters, however, deteriorate at low flow rates, because signals picked up by the sensors in these cases become weak and vortex frequencies are difficult to be extracted from the sensor signals. If the performance of vortex flowmeters at low flow rates is improved or the lower measurement limit is extended, the application range of vortex flowmeters will be widened considerably.

Efforts to extend the lower measurement limit of vortex flowmeters have been made for decades. The techniques employed in these efforts can be mainly divided into three categories: adoption of sensitive signal pick-up methods, application of advanced signal processing algorithms, and use of dual or multiple bluff bodies.

Barton and Saoudi used the multimode optical fiber as bluff body and detected the vortex frequency from the intensity modulation [3]. Hans and Windorfer applied ultrasound to vortex flowmeters with improved sensitivity [4]. These approaches may complicate the manufacture of the vortex flowmeter and lead to additional costs. Zhang *et al* extended the lower measurement limit of vortex flowmeters through wavelet-transform-based denoising [5]. Sun *et al* improved the anti-disturbance ability of vortex flowmeters by applying the Hilbert-Huang transform to the vortex signal processing [6]. Xu *et al* developed two kinds of digital signal processing systems to improve the accuracy of the output pulse of vortex flowmeters [7]. Advanced signal processing techniques can improve the ability to extract vortex frequencies from noisy signals, but real-time measurements are hard to achieve. Fu and Yang developed a dual bluff body vortex flowmeter with good noise immunity and improved sensibility [8]. Peng *et al* also proposed a dual bluff body vortex flowmeter with good

Article history: received on Jul. 18, 2010; accepted on Feb. 16, 2011; available online on Mar. 21, 2011; DOI: 10.2478/v10178-011-0012-5.

sensitivity and range ability [9]. In the dual bluff body vortex flowmeter, one more bluff body is used, so the pressure loss due to the vortex shedding rises.

This paper introduces the converging-diverging (C-D) structure into the vortex flowmeter to extend the lower limit of measurement. The bluff body is embedded in the C-D structure, and a new type of compact flow measurement device, the C-D vortex flowmeter, is proposed. Unlike the three categories of approaches mentioned above, the C-D vortex flowmeter can be used as a conventional vortex flowmeter without special requirements to signal pick-up, signal processing, and even installation conditions. The basic properties of the C-D vortex flowmeter are analyzed, and then the effects of bluff body shapes on the Strouhal number and the drag coefficient are also discussed.

2. Design principle

The C-D vortex flowmeter consists of a converging tube, a throat tube and a diverging tube, with a bluff body mounted in the throat tube, as shown in Fig.1. Denote the average fluid velocity and the inner diameter at the entrance of the converging tube as v_1 and D_1, and denote the average fluid velocity and the inner diameter of the throat tube as v_2 and D_2, it yields

$$D_1^2 v_1 = D_2^2 v_2 , \tag{1}$$

which is deduced from the continuity equation of fluids.

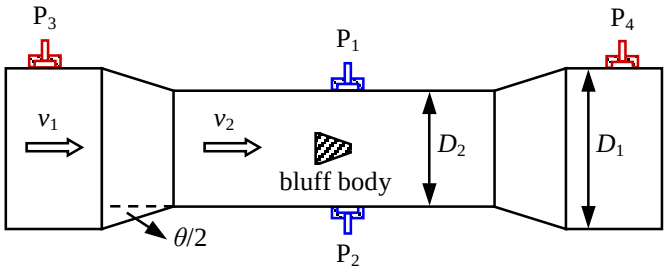

Fig.1. Structure of C-D vortex flowmeter.

Eq.(1) shows that v_2 is greater than v_1 because of the convergence of flow passage. If the vortex sensor is placed in the throat tube, the lower limit of measurement of the vortex flowmeter will be extended due to the increase of fluid velocity compared with that in front of the converging tube. This is the basic principle of the C-D vortex flowmeter whose lower limit of measurement can be extended markedly. If the C-D vortex flowmeter is well designed and manufactured as a compact device, it can be used as a conventional flowmeter without special requirements to installation conditions.

The convergence and divergence of tubes can be realized by linear or curved forms. The flow field behind a curved convergence is normally more uniform than that behind linear ones. The linear convergence, however, is preferred in most practical applications due to its simple manufacture and low cost. The ratio of D_1 to D_2 is normally restricted to less than two to avoid causing large pressure loss by the convergence. In addition to uniform flow field and small pressure loss, the most important factor in C-D vortex flowmeter design is to maintain a regular and stable vortex street in the throat tube. Moreover, the compactness of the whole device is also vital to practical applications. Therefore, the length of the throat tube and the converging angle need proper design and careful selection.

Metrol. Meas. Syst., Vol. XVIII (2011), No. 1, pp. 129-136

The optimal length of the throat tube is defined as the shortest length at which the vortex street can be generated and maintained regularly in the throat tube. For lack of theory on the optimal length of the throat tube, this parameter is determined mostly by trial and error based on experiments. The local resistance h_j of linear converging tubes is calculated by [10]

$$h_j = \zeta \frac{v_1^2}{2g}; \tag{2}$$

$$\zeta = k\left(\frac{1}{\varepsilon} - 1\right)^2 + \frac{\lambda}{8\tan\frac{\theta}{2}}\left(1 - \frac{D_2^4}{D_1^4}\right); \tag{3}$$

$$\varepsilon = 0.57 + \frac{0.043}{1.1 - \frac{D_2^2}{D_2^2}}, \tag{4}$$

where ζ is the local resistance coefficient, λ is the frictional drag coefficient, θ is the converging angle, ε and k are experimental coefficients. By comparing the local resistances at various converging angles according to Eqs.(2) – (4), it is found that the minimum local resistance is reached when $\theta = 40°$.

3. Experiments

Experiments were conducted with air under normal laboratory conditions to evaluate the performance of the C-D vortex flowmeter designed. The experimental rig is composed mainly of five sonic nozzles and the C-D vortex flowmeter, as shown in Fig.2.

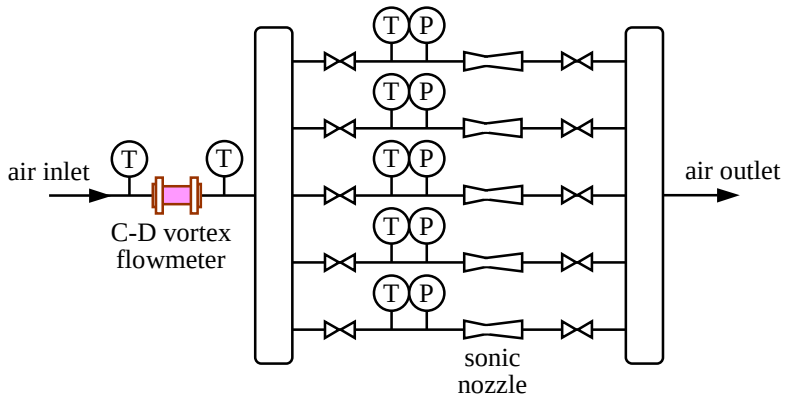

Fig.2. Experimental rig.

The sonic nozzles were used as the standard flow rate device. When their valves were fully opened, the five sonic nozzles corresponded to the flow rate of 10, 20, 40, 60, and 80 $m^3 \cdot h^{-1}$, respectively. The flow rate through the system was calculated from the valves fully opened. A variety of flow rates, from 10 to 210 $m^3 \cdot h^{-1}$, could be obtained by adjusting the combination of the sonic nozzles. The measurement uncertainty of the flow rate obtained from the sonic nozzles was 1%, calibrated by the manufacturer.

The C-D vortex flowmeter for the experiments is shown in Fig.1. The inner diameters D_1 and D_2 were 36 mm and 50 mm. The reason for choosing these two values is that the average fluid velocity in the 36-mm tube is just twice of that in the 50-mm tube, and it is convenient for comparison and discussion. The upstream and downstream straight pipes connecting the

C-D vortex flowmeter were both $25D_1$ long. Under the experimental conditions, the shortest or optimal length of the throat tube that generated stable vortices was $4D_2$ at the converging angle $\theta = 40°$ by trial and error. The bluff body was mounted at the center of the throat tube. The shapes of the tested bluff bodies included trapezoid and square, both with the width of 10 mm.

The vortex signals were obtained by the Duct-wall Differential Pressure Method (DDPM) [11,12]. The differential wall pressures behind the bluff body were measured by a Honeywell 24PC sensor. The two tags P_1 and P_2 connected with 24PC through sampling tubes were situated symmetrically on the tube wall and were $0.2D_2$ downstream of the front surface of the bluff body. The output of 24PC was acquired by a Tektronix TDS 430A digital oscilloscope. The pressure losses caused by the convergence and divergence of tubes were measured by a Keller PD-23 transmitter and were recorded by a computer. The two tags P_3 and P_4 for the pressure loss measurement were located 15 mm respectively from the entrance and the outlet of the C-D vortex flowmeter. The sampling frequency of all the pressure signals was 1000 Hz, and the duration time was 10 s.

4. Results and discussion

4.1. Basic performance of the C-D vortex flowmeter

At flow rates from 10 to 140 $m^3 \cdot h^{-1}$, experiments were carried out on the C-D vortex flowmeter with a trapezoidal bluff body to test the basic performance improved through the converging-diverging structure. The differential wall pressure measured by the 24PC sensor was stored, from which the vortex frequency f was extracted by Fourier analysis. Fig.3 shows the relationship between the vortex frequency f and the average fluid velocity v_2 in the throat tube. Fig.4 presents the relationship between the Strouhal number St and the average fluid velocity v_2 in the throat tube.

The average fluid velocity v_2 in the throat tube and the Strouhal number St were

$$v_2 = \frac{4Q}{\pi D_2^2}; \tag{5}$$

$$St = \frac{fd}{v_2}. \tag{6}$$

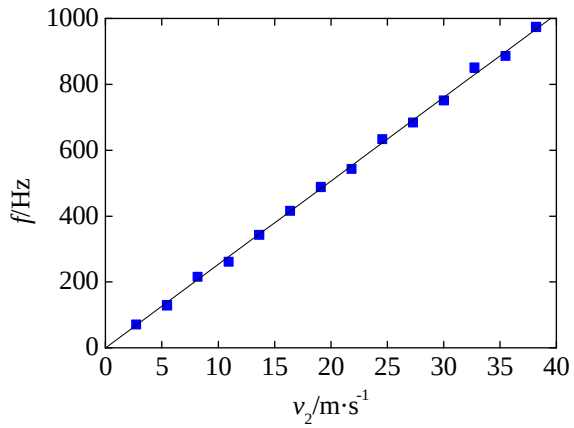

Fig.3. Vortex frequency versus average flow velocity in the throat tube.

Metrol. Meas. Syst., Vol. XVIII (2011), No. 1, pp. 129-136

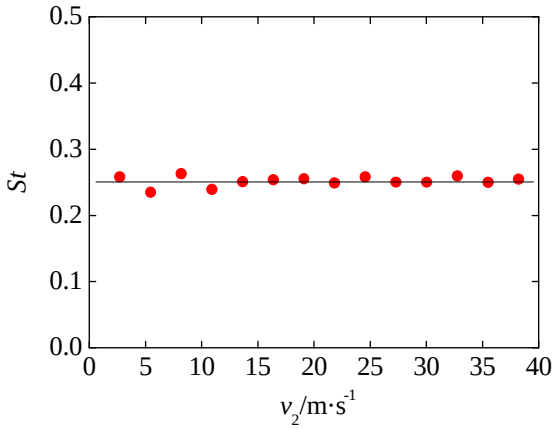

Fig.4. Distribution of Strouhal number versus Reynolds number.

Fig.3 shows good linearity in the f–v_2 relationship, and Fig.4 shows St is nearly constant at 0.25. The nonlinearity in the f–v_2 relationship is ± 5.6%. These results imply that there exist regular and stable vortex streets in the throat tube. The flow rate in the pipe, therefore, can be obtained from the vortex frequency. The formula of flow measurement based on the theory of Karman vortex street seems still tenable in the C-D structure properly designed. The average fluid velocity v_2 in the throat tube was 2.73 to 38.22 m·s^{-1} during the experiments, so the average fluid velocity v_1 at the entrance of the converging tube was 1.37 to 19.11 m·s^{-1} correspondingly. Compared with the lower limit of measurement (v = 2.78 m·s^{-1}) of DDPM-based vortex flowmeters without convergence and divergence [13], a 51% extension of the lower limit of measurement was achieved by the C-D structure. It also indicates that the C-D vortex flowmeter can provide a solution to the flow measurement of low-velocity fluids.

4.2. Effect of bluff body shape

The bluff body is the core part of a vortex flowmeter. The discharge characteristics of a vortex flowmeter are closely related to the shape of the bluff body. However, there is lack of theoretical foundation for the design of optimal bluff body shapes. Bluff bodies with shape edges have good mechanical properties to generate intensive vortex shedding and have been widely adopted in vortex flowmeters.

After having established the basic structure of the C-D vortex flowmeter, the effects of the bluff body shape on the Strouhal number and the drag coefficient are discussed in this section. The shapes of the tested bluff bodies included the trapezoid and square, both with the width of 10 mm. The structure and geometric dimensions of the bluff bodies are shown in Fig.5.

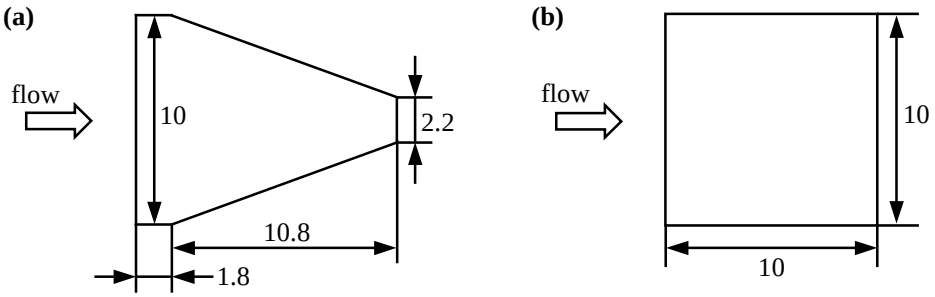

Fig.5. Structure of bluff bodies (unit: mm): (a) Trapezoidal shape; (b) Square shape.

At the flow rates from 10 to 140 $m^3 \cdot h^{-1}$, the differential wall pressure output from the C-D vortex flowmeters respectively with a trapezoidal and a square bluff body were measured and transformed to the frequency domain, and then the vortex frequencies were obtained. Fig.6 shows the relationship between the Strouhal numbers and the average fluid velocities in the throat tube for the trapezoidal and square bluff bodies. The Strouhal numbers of both bluff bodies are constant on the whole, but the Strouhal number of the trapezoidal bluff body is slightly greater than that of the square bluff body under the same fluid velocity. Moreover, the invariability of the Strouhal number of the trapezoidal bluff body is better than for the square one, especially at v_2 less than 10 $m \cdot s^{-1}$.

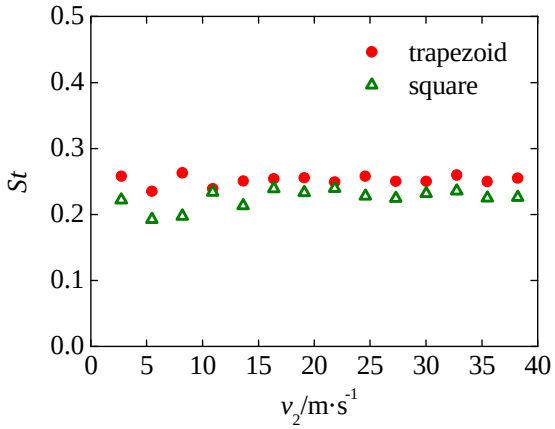

Fig.6. Strouhal numbers of different bluff bodies.

Pressure loss is one of the most important factors in the selection of flow measurement devices. For a C-D vortex flowmeter, additional pressure loss arises due to the C-D structure besides the pressure loss caused by the bluff body. Therefore, the pressure loss should be considered carefully, and is used as an indicator to evaluate the performance of C-D vortex flowmeters. The drag coefficient is a dimensionless parameter to describe the pressure loss of fluid flows, and its definition is as follows:

$$C_D = \frac{2\Delta p}{\rho v_2^2}. \tag{7}$$

At flow rates from 10 to 140 $m^3 \cdot h^{-1}$, the pressure losses of the trapezoidal and square bluff bodies were measured from the tags P_3 and P_4 by the Keller PD-23 transmitter, and the average value of each pressure loss time series acquired was adopted as Δp to calculate C_D using Eq.(7). The relationship of the drag coefficients and the average fluid velocities in the throat tube for the trapezoidal and square bluff bodies is shown in Fig.7. The relations between the drag coefficient and the average fluid velocity in the throat tube of the trapezoidal and square bluff bodies are basically uniform, but the drag coefficient of the trapezoidal bluff body is less than that of the square one at the same fluid velocity. For both bluff bodies, moreover, when v_2 is less than 10 $m \cdot s^{-1}$, the drag coefficient decreases markedly with the fluid velocity; when v_2 is greater than 10 $m \cdot s^{-1}$, the drag keeps nearly constant.

Metrol. Meas. Syst., Vol. XVIII (2011), No. 1, pp. 129-136

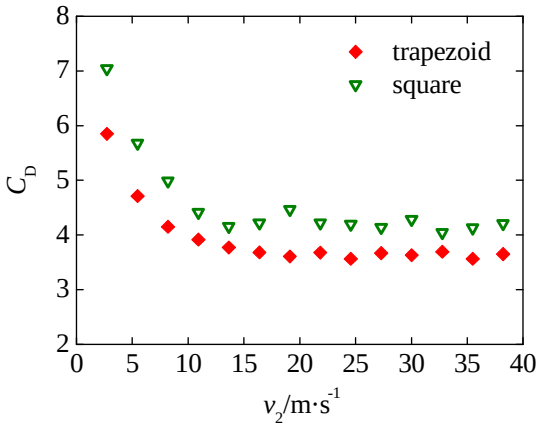

Fig.7. Drag coefficients of different bluff bodies.

From the above discussion, it suggests that the trapezoidal bluff body is more suitable for the C-D vortex flowmeter. The reasons can be explained from the view of fluid mechanics. The processes of the velocity decrement and the pressure increase of the fluid are smooth and steady near the trapezoidal bluff body due to its two sloped edges, along which the boundary layers develop gradually if the slope angle is designed appropriately. Under such circumstances, the vortex signals are intensive and stable, and the effects of the fluid disturbance will be reduced reasonably. Thus, the vortex frequency is to be easily extracted from the differential wall pressure signals and the flow rate is obtained with high accuracy.

5. Conclusions

The idea of using the C-D structure is proposed to extend the lower limit of measurement of vortex flowmeters. The C-D vortex flowmeter is designed as a compact device compared with conventional ones, and has no special requirements to the installation. The performance of the C-D vortex flowmeter is tested experimentally and the effect of the bluff body shape is analyzed. Major findings are summarized as follows:

(1) The lower limit of measurement of vortex flowmeters can be extended through the C-D structure. A 51% extension of the lower limit of measurement is realized by the present design, compared with vortex flowmeters without convergence and divergence using the same vortex frequency acquisition technique.

(2) By comparing the overall performance of the trapezoidal and the square bluff bodies, the trapezoidal one is recommended to be used in the C-D vortex flowmeter, because it has a larger Strouhal number and smaller pressure loss.

However, some questions still remain open for further investigations. For example, the optimal length of the throat tube should be determined more precisely, either by experiments or by numerical simulations.

Acknowledgements

This work is supported by the National Natural Science Foundation of China (51006125), the China Postdoctoral Science Foundation (200801346, 20100471227), and the Postdoctoral Science Foundation of Central South University. The author thanks Professor Hongjian Zhang of Zhejiang University for his advice and suggestions on undertaking the research as reported in the paper.

References

[1] Shakouchi, T., Tian, D., Ida, T., Nakamura, T. (2001). Measurement of flow rates of gas-liquid two-phase flow by Karman vortex. *Proceedings of the 3rd International Symposium on Measurement Techniques for Multiphase Flows.* Fukui. Japan, 83–89.

[2] Sun, Z., Zhang H. (2010). Measurement of the flow rate and volume void fraction of gas-liquid bubble flow using a vortex flow meter. *Chemical Engineering Communications*, 197(2), 145–157.

[3] Barton, J., Saoudi, M. (1986). A fiber optic vortex flowmeter. *Journal of Physics E: Scientific Instruments*, 19(1), 64–66.

[4] Hans, V., Windorfer, H. (2003). Comparison of pressure and ultrasound measurements in vortex flow meters. *Measurement*, 33(2), 121–133.

[5] Zhang, T., Sun, H., Peng, W. (2004). Wavelet denoising applied to vortex flowmeters. *Flow Measurement and Instrumentation*, 15(5–6), 325–329.

[6] Sun, Z., Zhou, J., Zhou, P.(2006). Application of Hilbert-Huang transform to denoising in vortex flowmeter. *Journal of Central South University of Technology*, 13(5), 501–505.

[7] Xu, K., Zhu, Z., Zhou, Y., Wang, X., Liu, S., Huang, Y., Chen Z. (2009). Applied digital signal processing systems for vortex flowmeter with digital signal processing. *Review of Scientific instruments*, 80(2), 025104.

[8] Fu, X., Yang, H. (2001). Study on hydrodynamic vibration in dual bluff body vortex flowmeter. *Chinese Journal of Chemical Engineering*, 9(2), 123–128.

[9] Peng, J., Fu, X., Chen, Y.(2004). Flow measurement by a new type vortex flowmeter of dual triangulate bluff body. *Sensors and Actuators. A: Physical*, 115(1), 53–59.

[10] Mo, N. (2000). *Engineering Fluid Mechanics*. Huazhong University of Science and Technology Press. Wuhan. (in Chinese).

[11] Sun, Z., Zhang, H., Zhou, J. (2007). Investigation of the pressure probe properties as the sensor in the vortex flowmeter. *Sensors and Actuators. A: Physical*, 136(2), 646–655.

[12] Sun, Z., Zhang, H., Zhou, J. (2008). Evaluation of uncertainty in a vortex flowmeter measurement. *Measurement*, 41(4), 349–356.

[13] Sun, Z., Zhang, H., Huang, Y., Han X. (2006). Impact analysis of vortex flowmeter measured with duct-wall differential pressure method. *Journal of Zhejiang University. Engineering Science*, 40(12), 2103–2106 (in Chinese).